ACS OMEGA

Open Access

http://pubs.acs.org/journal/acsodf

Article

Effect of Pyrolysis Temperature on the Physicochemical Properties and Structural Characteristics of Agricultural Wastes-Derived Biochar

Kowsalya Sathyabama and Saiyyeda Firdous*

Cite This: https://doi.org/10.1021/acsomega.5c00120

Read Online

ACCESS | Metrics & More | Article Recommendations

ABSTRACT: The efficient handling of agricultural waste is rapidly gaining worldwide recognition. This study analyzes the impact of three distinct pyrolysis temperatures (250, 300, and 350 °C) on the physicochemical properties of the biochar produced from rice husk, sugarcane bagasse, and groundnut shells with a fixed pyrolysis time of 3 h. The influence of the pyrolysis temperature was assessed by calculating the biochar yield, electrical conductivity (EC), pH, proximate analysis, and ultimate analysis. Further structural and morphological characterization was performed using Fourier transform infrared spectroscopy (FTIR), scanning electron microscopy (SEM), ζ-potential analysis, and X-ray diffraction (XRD). The physicochemical properties are influenced by the feedstock materials and the temperature during the pyrolysis process. Increasing the pyrolysis temperature leads to a rise in the ash content (39.12%), fixed carbon content (82.4%), EC (0.56 to 4.567 dS/m), and pH (4.0 to 7.7). In contrast, yield, moisture, and volatile matter exhibited a decreasing trend; biochar yield dropped by more than 50% across all feedstocks; moisture content diminished by up to 3.4%, and the volatile matter decreased to 6.9% at elevated temperatures. Elemental analysis indicated the highest carbon content at 350 °C in all samples, increasing up to 75.56%, while elements such as nitrogen, hydrogen, sulfur, and oxygen content and atomic ratio decreased. Inductively coupled plasma mass spectrometry (ICP-MS) analysis shows a higher concentration of minerals, such as potassium, calcium, and magnesium, at higher temperatures. SEM results indicate a well-defined pore structure at moderate thermal conditions of 300 and 350 °C. FTIR and XRD characterization suggests the presence of various functional groups and crystalline structures, respectively. Biochar exhibited more negative ζ-potential values at higher temperatures (350 °C), ranging from −36.4 to −59.3 mV, indicating a high electrostatic interaction with cations, heavy metals, and pollutants. This research offers a unique and comprehensive analysis of three different agricultural feedstocks subjected to moderate pyrolysis conditions, providing new insights into improving biochar properties for soil remediation and environmental sustainability.

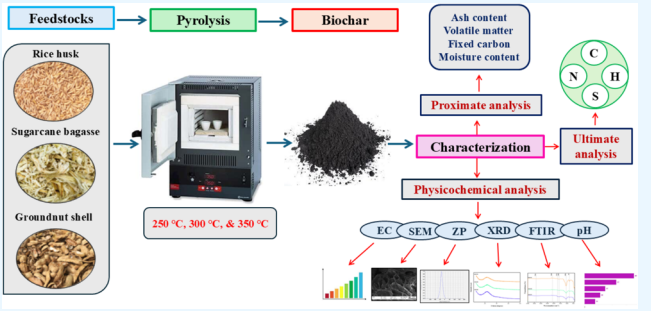

1. INTRODUCTION

As India is primarily an agrarian nation, the progress of its socioeconomic status is highly dependent on the agricultural methods that result in crop residues. The Ministry of New and Renewable Energy statistics report (2019) states that India generates around 500 million tonnes of crop residues annually.[1] 140 million tons of crop residues are not being utilized. However, they can be used for feeding animals, constructing roofs for rural homes, cooking, fuel, and industrial purposes, whereas in open fields, 92 million tons of crop residues were burned.[2,3] Clearing agricultural crop residues by burning is a simple and cost-effective method for clearing and preparing land for the next crop season. However, it results in a significant disparity in the carbon being released into and the uptake of carbon from the atmosphere.[4,5] The annual increase in atmospheric carbon dioxide (CO_2) is estimated at 4.1×10^9 tons per year (IPCC, 2007). It is closely linked with agricultural activities responsible for the rise in atmospheric CO_2 levels, the depletion of soil carbon, and other climate change-related issues.[6] Incinerating crop residues in agricultural fields results in numerous detrimental effects, encompassing air pollution, elevation of greenhouse gas (GHG) emissions, and plant nutrient loss. Punjab is facing significant alarming issues, i.e., around 70−80 million tons of rice and wheat straw is burned each year, leading to the emission of approximately 140 million tons of CO_2, methane, nitrous oxide, etc. into the atmosphere.[7] These agricultural crop

Received: January 6, 2025
Revised: July 8, 2025
Accepted: July 9, 2025

residues are often discarded as waste with minimal or no economic worth, leading to expensive disposal and potential environmental consequences.[8]

To tackle these issues, transforming agricultural residue into biochar paves the way for a good alternative to conserve natural resources and safeguard the environment. Recent studies on the effect of biochar in various soil types have shown promising results on plant growth and soil characteristics.[9] Biochar is a porous, carbon-rich (70−80%), black, solid, fine-grained structure prepared through the thermal breakdown (300−850 °C) of agricultural wastes like biomass, wood waste, and manures in the absence of oxygen.[10]

Biochar properties and characterization rely on the parameters of pyrolysis (pressure, temperature, and heating rate, etc.). Biochar production involves the use of different methods: pyrolysis, hydrothermal gasification, and torrefaction.[11] The higher porosity of biochar explains its extensive surface area, which tends to increase as the pyrolysis temperature rises, up to approximately 850 °C. The biochar application improves soil fertility, thereby increasing agricultural productivity. Additionally, the soil characteristics, including both physical and chemical properties, are improved, such as its structure, porosity, pH level, cation exchange capacity (CEC), water absorption, and nutrient retention.[6,12] Solid biomass, being mainly composed of organic waste, holds significant potential for biochar production.[13]

Accessing biochar surface functionalization, stability, structure, and elemental composition is crucial for understanding the characterization of biochar. Ash, carbon, and elements constitute the primary contents of biochar. Scanning electron microscope (SEM) is utilized to observe structural features of biochar, Fourier transform infrared spectroscopy (FTIR) is employed to study its surface chemical functionalities, thermogravimetric analysis (TGA) is conducted to analyze its chemical composition, X-ray diffraction analysis (XRD) is used to obtain detailed information about its physical properties, dynamic light scattering system (DLS) is employed to measure particle size distribution and ζ-potential, Brunauer−Emmett−Teller (BET) analysis is carried out to assess its surface area, biochar porosity and elemental composition were studied using CHNS analysis, and nuclear magnetic resonance (NMR) is utilized to analyze its molecular structure at the atomic level.[11,14]

This study aims to investigate the effects of different pyrolysis temperatures on biochar produced from three widely used agricultural residues, such as rice husk, sugarcane bagasse, and groundnut shell, employing a broad range of physicochemical and morphological assessments. In contrast to most of the previous research that typically focuses on single feedstock or relies on high temperatures, this study provides a comparative assessment of biochar at moderate pyrolysis temperatures (250−350 °C) relevant to low-cost biochar production. The novelty of this work lies in identifying the optimal pyrolysis conditions to synthesize biochar with specific and desirable properties.

2. MATERIALS AND METHODS

2.1. Site of Research. This study was performed at Vellore Institute of Technology (VIT), Vellore, Tamil Nadu, India.

2.2. Feedstock Collection and Preparation. Three distinct agricultural biomass materials were utilized as raw materials for biochar production. Rice husk (RH), sugarcane bagasse (SB), and groundnut shell (GS) were chosen for the study. These samples were collected from the nearby regions of Vellore, Tamil Nadu, India. Samples were thoroughly cleaned to eliminate traces of dirt, sand, or unwanted substances. The raw materials were initially placed under shaded conditions to expel the initial moisture content, after which they were cut into small fragments using sanitized scissors. The drying of samples was carried out for 2 h at 65 °C in a hot-air oven, ensuring no weight change was observed. This process helps to eliminate any residual moisture that may persist after preliminary shade drying. The desiccated samples were pyrolyzed at three distinct temperatures for 3 h (250, 300, and 350 °C). The chosen temperatures were determined from previous studies showing that pyrolysis at moderate temperatures produces biochar with advantageous characteristics, including improved nutrient retention and structural integrity, while also being economically viable for practical applications.[15,16] The furnace underwent charring, maintaining a nitrogen flow in an inert environment. Following the pyrolysis, the biochar samples were gathered after cooling of the furnace at ambient temperature and stored in a desiccator. Using a mortar and pestle, biochar was made into fine powder and stored in an airtight container for further testing, which was carried out in triplicate.

2.3. Yield of Biochar. The biochar yield is strongly correlated to pyrolysis temperatures. Higher temperatures lead to greater thermal degradation through condensation, dehydration, and gasification. Therefore, the production of biochar at higher temperatures is lower than that at lower temperatures. According to Sahoo et al.,[4] the yield of biochar can be calculated using eq 1

$$\text{yield of the biochar (\%)} = \frac{\text{mass of biochar}}{\text{mass of the raw material}} \times 100 \quad (1)$$

2.4. Electrical Conductivity (EC) and pH. A 1:20 ratio of biochar and deionized water was prepared and stirred for 1.5 h to reach equilibrium before analysis.[12] The EC and pH values were measured with a benchtop V Tech conductivity meter and a Systronics pH meter (digital)[17].

2.5. Proximate Analysis. Using proximity analysis, the ash content, volatile matter content, moisture content, and fixed carbon content were assessed. One gram of biochar samples was placed in a preweighed ceramic crucible after being dried in a hot-air oven and then exposed to a temperature of 750 °C for 6 h.[12] After cooling, the remaining ash was weighed and the ash content was calculated using eq 2

$$\text{ash (\%)} = \frac{\text{mass of residue after heating to 750 °C}}{\text{initial mass of biochar}} \times 10 \quad (2)$$

To calculate the moisture percentage of the biochar, 1 g of air-dried biochar samples was subjected to 105 °C for 2 h. The moisture content (%) was determined according to eq 3

https://doi.org/10.1021/acsomega.5c00120
ACS Omega XXXX, XXX, XXX−XXX

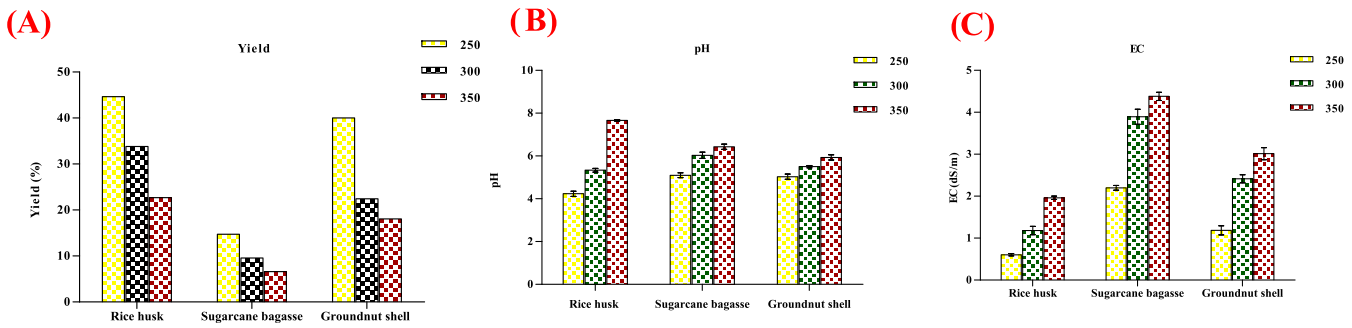

Figure 1. Effect of temperature on the yield (A), pH (B), and electrical conductivity (C) of the biochar produced from rice husk, sugarcane bagasse, and groundnut shell at different temperatures (250, 300, and 350 °C).

$$(\%)\ \text{moisture} = \frac{(\text{mass of air dried sample} - \text{mass of sample after drying at 105 °C})}{\text{mass of air dried sample}} \times 100 \quad (3)$$

To ascertain the volatile components of the biochar, 1 g of oven-dried biochar was accurately weighed and burned at 750 °C for 11 min.[18] Equation 4 was used to calculate the volatile content (in %),

$$\text{VM}\ (\%) = \frac{\text{oven dried sample mass} - \text{sample mass after heating to 750 °C}}{\text{mass of oven dried sample}} \times 100 \quad (4)$$

The overall carbon content of the biochar was calculated using eq 5 as follows

$$(\%)\ \text{fixed carbon} = 100 - (\text{moisture content}\ (\%) + \text{ash}\ (\%) + \text{volatile matter}\ (\%)) \quad (5)$$

2.6. Elemental Analysis. The composition of elements such as carbon (C), hydrogen (H), nitrogen (N), and sulfur (S) was analyzed using the elemental analyzer (PerkinElmer 2400 Series II) in CHNS analysis mode. Oxygen (%) was determined by measuring the difference between the sum of the ash contents, C, H, N, and S, from 100. The elemental values were used to determine the atomic ratio of the biochar samples.[14,15] The predominant biochar inorganic elements were isolated using the double acid digestion method, for which a 7:3 ratio (nitric acid:hydrogen peroxide) was used. Analysis was done using a Three Quad-NexION 1000 inductively coupled plasma mass spectrometer[19−21].

2.7. Characterization of Biochar. *2.7.1. SEM.* The surface structure of biochar and the composition of elements were studied by using a CARL ZEISS EVO 18 scanning electron microscope with energy-dispersive X-rays (EDX). The surface topography of the biochar and its complex porous architecture contribute significantly to the adsorption properties. In this examination, biochar specimens were coated with a platinum/gold coating to minimize the charging during analysis. The SEM images were taken at different magnifications between 50× and 15,000×.

2.7.2. FTIR. The intrinsic chemistry of the biochar and the various functional elements were analyzed using IR Affinity-1, Thermo Nicolet iS50 Fourier transform infrared spectroscopy (Shimadzu, Japan, Thermo Fisher Scientific) in KBr mode, encompassing an infrared spectral range extending from 4000 to 500 cm^{-1}.

2.7.3. XRD. The biochar sample's crystalline nature was examined using a Bruker D8 advanced X-ray diffractometer (Panalytical X'Pert3, Germany, Netherlands) with a diffraction angle range of 1−80°.

2.7.4. ζ-Potential. A ζ-potential analyzer (Litesizer 500; made by Anton Paar GmbH, Austria) was utilized to assess the electrical charge surrounding the particles. As stated by Gamal et al., biochar precipitation was prepared with a ratio of water to biochar of 0.1 g to 200 mL, at a concentration of 0.05%, and its ζ-potential was determined after being shaken for 12 h at 150 rpm.

3. RESULTS AND DISCUSSION

3.1. Yield, pH, and Electrical Conductivity (EC). The biochar yield from rice husks (RH), sugarcane bagasse (SB), and groundnut shells (GS) at 250, 300, and 350 °C is shown in Figure 1A. Data shows a diminish in biochar upon an increase in the temperature required for pyrolysis. The maximum biochar production was measured at 250 °C, yielding 44.63% for RH, 14.72% for SB, and 40.00% for GS. When the temperature increased from 300 to 350 °C, the yield of RH, SB, and GS biochar decreased from 33.83 to 22.69%, from 9.58 to 6.62%, and from 22.43 to 18.06%, respectively. This reduction is because of the intense release of volatiles and thermal decomposition at higher temperatures.[24] The results are consistent with the results of Tomczyk et al.,[16] which states that a higher pyrolysis temperature improves the devolatilization, leading to a lower yield, as the volatile components are degraded to a lesser extent. The higher the thermal conditions, the more pronounced the degradation, which leads to a reduction in solid residues and consequently reduces the yield of the biochar.

Biochar produced with a higher pyrolysis temperature has a higher pH (Figure 1). As the temperature range increases, the pH also increases, indicating the depletion of acidic functional groups and the development of mineral phases containing

https://doi.org/10.1021/acsomega.5c00120
ACS Omega XXXX, XXX, XXX−XXX

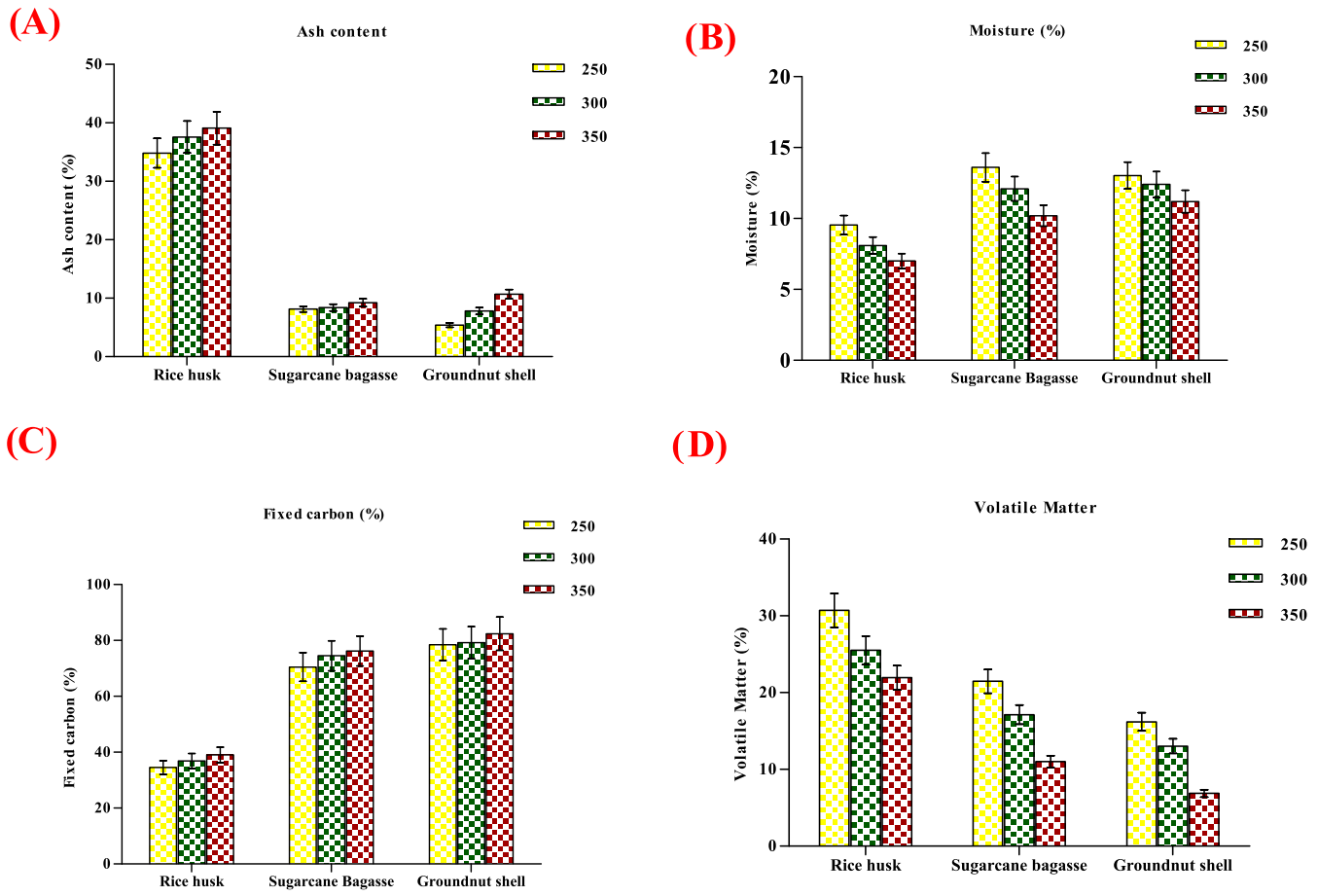

Figure 2. Effect of different temperatures (250, 300, and 350 °C) on ash (A), moisture content (B), fixed carbon (C), and volatile matter (D).

calcium (Ca), magnesium (Mg), sodium (Na), and potassium (K) in the form of oxide, hydroxide, and carbonate minerals. Elevated thermal conditions promote the breakdown of organic acids while enhancing the mineral composition within the biochar, resulting in substances that exhibit greater alkalinity and conductivity.[25] The change in pH with the elevation of pyrolysis temperature from 250 to 350 °C has been observed in feedstocks and the data revealed an increase in pH from 4.0 to 7.7 in rice husks, 4.8 to 6.6 in sugarcane bagasse, and 4.8 to 6.1 in groundnut shells, along with rise in the pyrolysis temperature. According to Dhar et al.,[18] elevating the pyrolysis temperature from 350 to 650 °C boosts the pH from 7.64 to 10.03. RH biochar obtained at 350 °C had the maximum pH (7.7), while the minimum pH (4.0) was observed at 250 °C from the RH biochar. An increase in EC occurs as the pyrolysis temperature increases from 250 to 350 °C. The EC increased from 0.56 to 2.290, 2.101 to 4.567, and 1.023 to 3.101 dS m^{-1} for rice husk, sugarcane bagasse, and groundnut shells, respectively, as the temperature rose from 250 to 350 °C (Figure 1C). The maximum EC (4.567 dS m^{-1}) was noticed at 350 °C for sugarcane bagasse, whereas the minimum conductivity (0.56 dS m^{-1}) was observed for rice husk at 250 °C. The results correspond with a study done by Conz et al.[26] in which the electrical conductivity of biochar correlates positively with the rise in pyrolysis temperature.

3.2. Proximate Analysis. Ash predominantly consists of inorganic minerals after pyrolysis of starting materials. High ash content in biochar is generally unfavorable because these inorganic minerals can clog the inner pores of the biochar and impair the absorbent characteristics. The fluctuation in the biochar ash content varies according to the feedstock type, pretreatment methods, temperature of pyrolysis, etc. According to Li et al.,[27] biochar usually contains 0.3 to 92.4% ash. The total biochar ash content ranged between 5.4 and 39.12%. The biochar sample from rice husk had the highest ash content (34.82 to 39.12%), followed by sugarcane bagasse (8 to 9.2%) and groundnut shells (5.4 to 10.7%). Based on these results, as the pyrolysis temperature increases from 250 to 350 °C, the ash content also increases. The highest ash content in rice husk was observed at 350 °C, possibly due to the raw material having rich minerals. Conversely, groundnut shells biochar at 250 °C had the lowest ash content (5.4%) (Figure 2A), which might be due to the lower amount of minerals in its raw materials. According to Bera et al.,[6] the rise in ash content concomitant with higher pyrolysis temperatures is associated with the amount of nonvolatile inorganic minerals remaining after the combustion of organic substances.[28]

The moisture content drops from 7 to 9.5%, 10.2 to 13.6%, and 11.2 to 13% in rice husk, sugarcane bagasse, and groundnut shells, respectively, as the temperature climbs from 250 to 350 °C during pyrolysis. SB250 had the maximum moisture content (13.6%), while RH350 had the minimum (7%) (Figure 2 B). The results agree with the study by Sahoo et al.[4] in which the moisture content decreased from 4.17 to 1.20% and from 6.22 to 6.04% for bamboo and pigeon pea stalks, respectively, when the temperature increased from 400 to 600 °C. As a result, elevated pyrolysis temperatures enhance the efficiency of water extraction due to augmented

https://doi.org/10.1021/acsomega.5c00120
ACS Omega XXXX, XXX, XXX−XXX

Table 1. CHNS and Atomic Ratio of Different Biochar Samples

sample code	C (%)	H (%)	N (%)	S (%)	O (%)	H/C	O/C	(O + N)/C
RH250	31.81	3.62	3.9	0.91	32.18	1.37	0.76	0.86
RH300	46.07	2.48	0.67	0.66	12.54	0.65	0.2	0.21
RH350	50.07	2.3	0.4	0.36	7.75	0.55	0.12	0.12
SB250	55.51	14.72	0.58	0.21	36.98	3.18	0.5	0.5
SB300	59.91	4.01	0.48	0.16	27.04	0.8	0.34	0.34
SB350	69.92	3.07	0.32	0.11	17.38	0.53	0.19	0.19
GS250	65.67	2.77	2.71	1.01	22.44	0.51	0.26	0.29
GS300	67.37	2.6	2.58	0.8	18.85	0.46	0.21	0.24
GS350	75.56	2.02	2.18	0.54	9	0.32	0.09	0.11

dehydration processes, yielding biochar that exhibits increased stability and hydrophobicity.

Figure 2C illustrates that the range of fixed carbon changes according to the raw material and pyrolysis temperature. The fixed carbon range rose from 34.47 to 38.96%, 70.5 to 79.8%, and 78.4 to 82.4% for rice husk, sugarcane bagasse, and groundnut shells, respectively, upon altering the temperature for pyrolysis from 250 to 350 °C. The maximum fixed carbon (82.4%) was observed in groundnut shells at 350 °C, and the minimum (34.47%) in rice husks at 250 °C. The increase in fixed carbon that occurs with rising temperatures aligns with the results reported by Sun et al.,[30] who established that thermal degradation at elevated temperatures encourages carbon enrichment and structural condensation. This results in biochars that are characterized by improved energy density and a higher ratio of aromatic carbon.

Figure 2D shows that the low pyrolysis temperature (250 °C) has more volatiles than the high temperature (350 °C). The range of volatile content was 30.7 to 21%, 21.5 to 11%, and 16.2 to 6.9% for rice husk, sugarcane bagasse, and groundnut shells, respectively. The reduction in the volatile content of the different biochars may be associated with the functional groups being present on the surface, e.g., O−C−O, CH, and insufficient carbonization.[4] A larger number of volatile contents was found in rice husks at 250 °C, while a smaller number of volatile contents was found in groundnut shells at 350 °C. The reduction of volatile matter is a characteristic outcome of pyrolysis conducted at elevated temperatures, as evidenced by the findings of Liu et al.,[29] which indicate that substantial devolatilization processes eradicate labile components and result in the residual formation of a more recalcitrant carbon structure. It emphasizes that higher pyrolysis temperatures lead to an increase in fixed carbon and a decrease in volatile content, which enhances the structural stability and long-term carbon storage potential of biochar in soil environments.[30,31] Additionally, higher ash content and improved thermal stability increase its effectiveness in heavy metal adsorption and remediation purposes.[29,16]

3.3. Elemental Analysis. The CHNS elemental analysis of rice husk (RH), sugarcane bagasse (SB), and groundnut shell (GS) biochar is shown in Table 1. The data indicate that the pyrolytic temperature positively correlated with the increase in carbon content, while the nitrogen, hydrogen, and sulfur content decreased. Carbon content was high in all biochar samples as the pyrolysis temperature increased from 250 to 350 °C. For RH biochar, the carbon content increased to 31.81 and 50.07% as the temperature shifted from 250 to 350 °C. Similarly, SB biochar's carbon content at 250 and 350 °C increased from 55.51 to 69.92%, respectively. GS biochar's carbon content ranged from 65.67 to 75.56% at 250 and 350 °C, respectively. The highest carbon content (75.56%) was found in GS350 and the lowest (31.81%) in RH250. This is due to the increasing carbonization reaction with increasing temperature and feedstock type. According to a study done by Novak et al.,[31] the removal of volatile substances by a high pyrolysis temperature causes an increase in the carbon content particularly of aromatic carbon, thereby improving stability and adsorption capacity. This is corroborated by the finding that the pyrolysis temperature changed from 250 to 350 °C, and the volatile matter content in the biochar samples dramatically dropped. The sulfur, oxygen, and hydrogen levels dropped as the temperature increased. As the pyrolysis temperature increased from 250 to 350 °C, the biochar hydrogen levels dropped from 3.62 to 2.30%, 14.72 to 3.07%, and 2.77 to 2.02% in RH, SB, and GS, respectively. Likewise, for RH, SB, and GS, the nitrogen concentration dropped from 3.09 to 0.40%, 0.58 to 0.32%, and 2.71 to 2.18%, respectively. The sulfur content sharply dropped at higher temperatures, with rice husk exhibiting the maximum sulfur content (0.91%) at 250 °C and, at 350 °C, the sulfur content decreased by 0.36%. Similarly, the sulfur content of sugarcane bagasse biochar was found to be highest (0.21%) at 250 °C and lowest (0.36%) at 350 °C. The sulfur concentration of groundnut shell biochar dropped from 1.01 to 0.54% with a rise in temperature from 250 to 350 °C, respectively. The observed decreases can be attributed to the thermal cleavage of bonds associated with the hydrogen, oxygen, and nitrogen, as Xiao et al.[33] showed that a decline in the H/C and O/C ratios with an increase in temperature signifies enhanced aromatization and structural condensation.

The determination of the atomic ratio of the biochar samples was performed by the percentage of their elemental composition, which served as an indicator of its possible interaction and polarity with water. The degree of aromaticity of biochar samples depends particularly on a factor known as the H/C ratio, while the hydrophilicity and polarity are related to factors known as (O/C) and (O + N)/C ratios. These atomic ratios are responsible for the interference compatibility between the surface of biochar and the polymer matrices. The biochar atomic ratio showed significant differences between feedstocks and pyrolysis temperature since there was a loss of both O and H atoms.[32] For different biochar samples, the values of O/C, H/C, and (O + N)/C ranged from 0.09 to 0.76, 0.32 to 3.18, and 0.11 to 0.86 in RH, SB, and GS biochar, respectively, at 250 to 350 °C. The results reveal that the atomic ratios decrease with increasing pyrolysis temperature. A similar result has been documented by Tomczyk et al.[16] that the atomic ratio decreased as the pyrolysis temperature increased. The reduction in the atomic ratio of H/C indicates increased aromatization and structural stability in the biochar

https://doi.org/10.1021/acsomega.5c00120
ACS Omega XXXX, XXX, XXX−XXX

Table 2. Inductively Coupled Plasma Mass Spectrometry (ICP-MS) Results

sample code	B11 (ppb)	Ca43 (ppb)	Co59 (ppb)	Cu63 (ppb)	Fe57 (ppb)	K39 (ppb)	Mg24 (ppb)	Mn55 (ppb)	Na23 (ppb)	Ni60 (ppb)	Pi31 (ppb)	Zn66 (ppb)
RH250	28.196	13.325	0.003	1.029	1.185	45.314	7.005	0.181	56.609	0.198	17.801	6.214
RH300	27.000	13.944	0.003	1.142	1.054	44.625	6.132	0.192	66.873	0.180	18.131	6.123
RH350	28.187	14.412	0.004	1.161	0.944	47.307	7.021	0.230	64.206	0.177	18.095	6.178
SB300	25.129	12.156	0.004	1.013	0.988	47.409	6.333	0.135	53.672	0.164	17.907	6.083
SB330	23.778	14.131	0.006	1.089	1.087	53.921	10.166	0.214	55.155	0.182	19.001	5.845
SB350	22.762	15.440	0.004	1.291	1.468	85.722	10.363	0.153	54.230	1.372	20.495	6.080
GS250	30.211	14.833	0.007	1.116	1.445	49.672	6.253	0.213	68.672	0.198	16.888	6.211
GS300	29.467	16.294	0.004	1.020	1.458	51.511	13.578	0.243	70.102	0.210	16.351	6.669
GS350	28.630	13.722	0.005	1.055	1.613	50.207	6.374	0.174	56.592	0.171	17.501	6.318

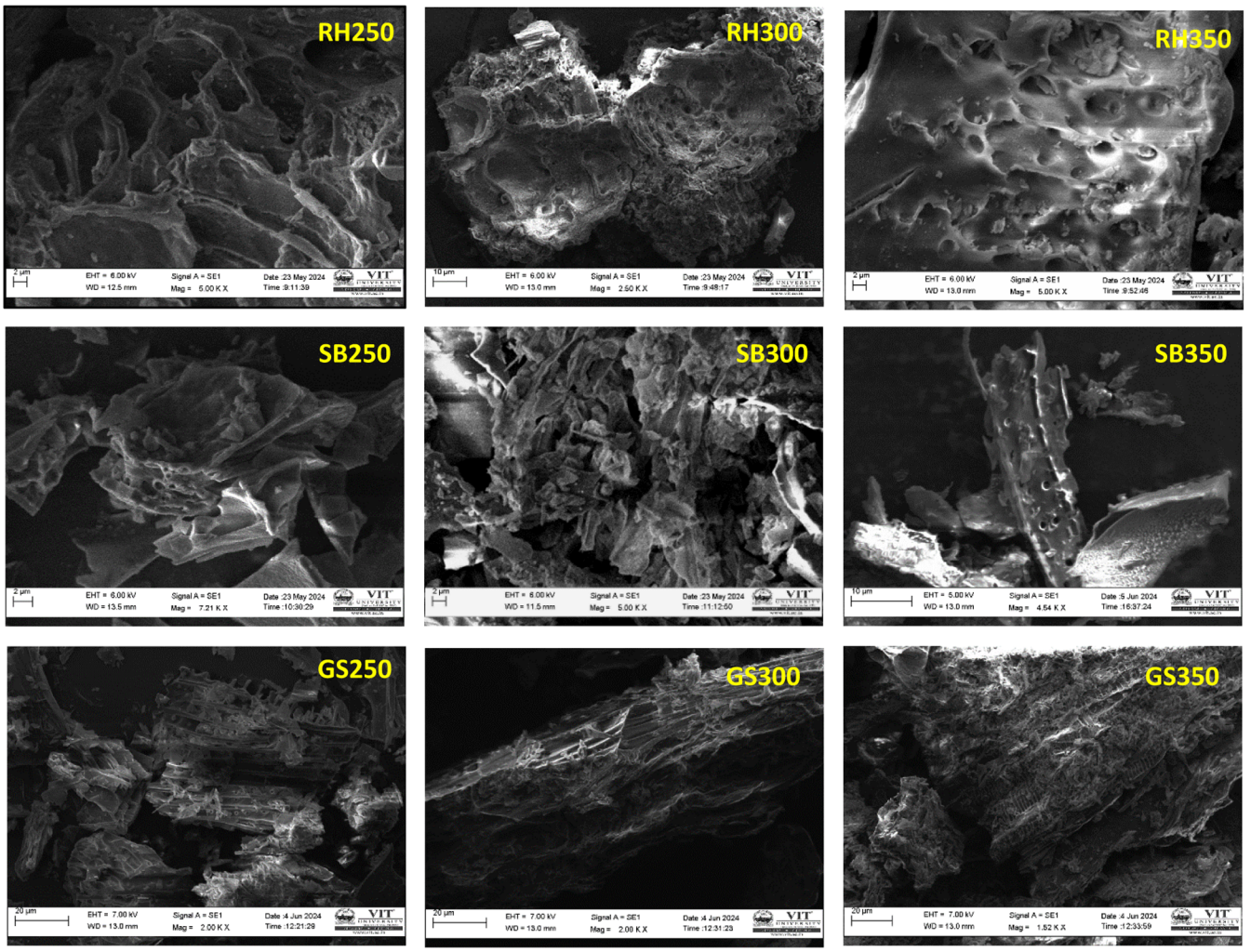

Figure 3. Scanning electron microscopic analysis of different biochars (rice husk, sugarcane bagasse, and groundnut shell) pyrolyzed at 250, 300, and 350 °C.

samples. The hydrogen loss caused by the dehydration and dehydrogenation processes can be associated with a decline in the H/C ratio as well as the breaking of weak interactions during the conversion of biochar. The ratio of the O/C and (O + N)/C decreases as the pyrolysis temperature rises. The oxygen functional group content in the biochar samples decreases when the pyrolysis temperature increases, as a result of the decrease in biochar hydrophilicity and polarity.[25] This indicates an increased level of aromaticity and chemical stability. These modifications improve the biochar's capacity to hold nutrients, interact with contaminants, and withstand microbial decomposition, thereby enhancing its effectiveness for uses such as adsorption, soil enhancement, and long-term carbon sequestration.[33,34]

ICP-MS data of rice husk, sugarcane bagasse, and groundnut shell biochar at 250, 300, and 350 °C shows that the boron concentration is stable in all samples and lies between 22.762 and 30.211 ppb. Depending on the pyrolysis temperature, the calcium concentration increased and reached a maximum value of 16.294 ppb in GS300. Cobalt is low in consistency in all samples and remained below 0.007 ppb. Potassium is essential for the physiological development of plants, and it is very high

https://doi.org/10.1021/acsomega.5c00120
ACS Omega XXXX, XXX, XXX−XXX

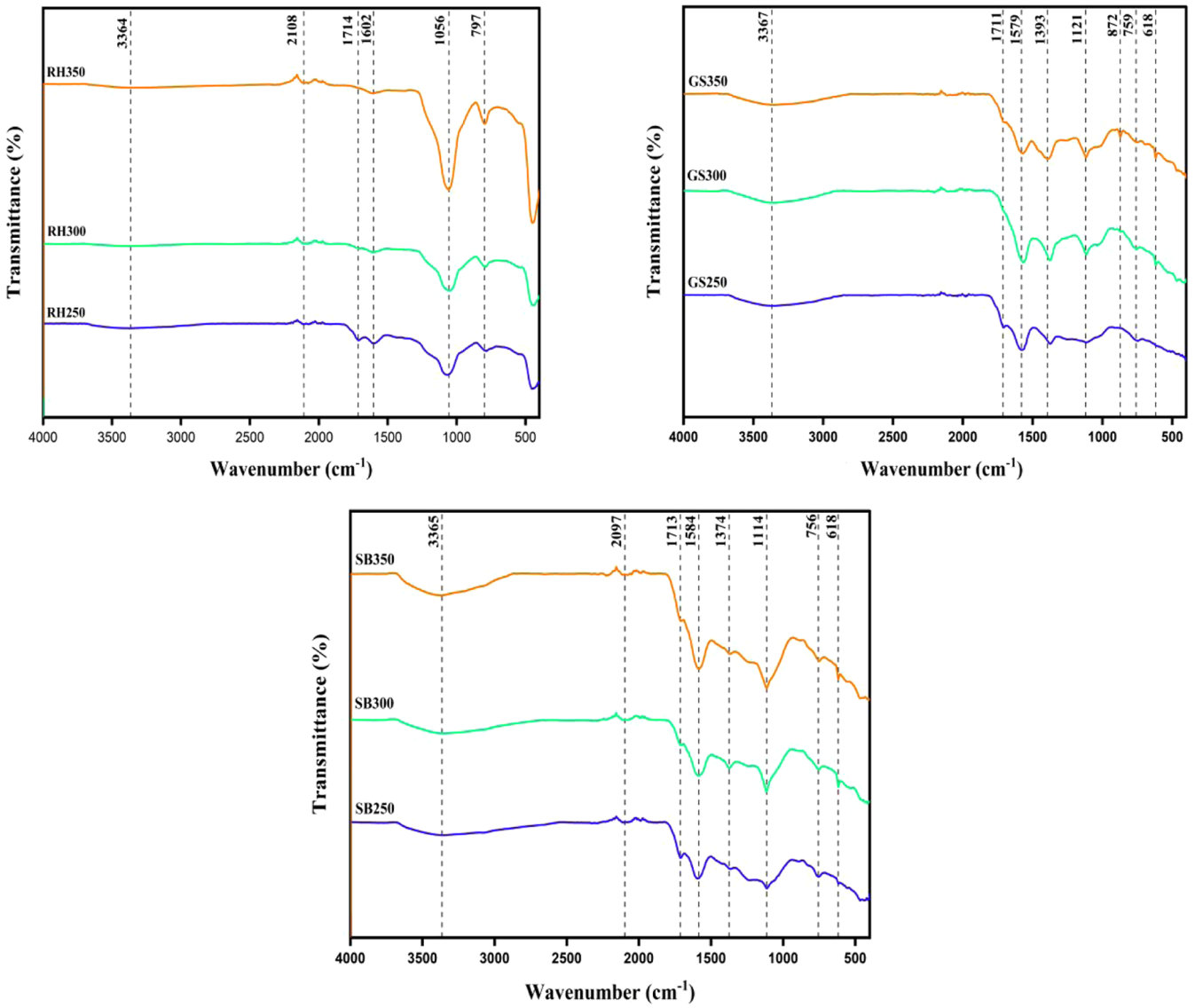

Figure 4. FTIR spectra of biochar samples.

in SB350 at 85.722 ppb (Table 2), suggesting that biochar synthesized at high pyrolytic temperatures may benefit agricultural purposes significantly. The concentrations of phosphorus and magnesium are comparatively stable, with a slight increase in temperature. The pyrolysis temperature determines the variation in the concentration of trace elements such as copper, cobalt, iron, nickel, and zinc, and it improves the retention of essential elements, particularly potassium, calcium, and magnesium, making biochar in the form of SB and GS at 350 °C particularly suitable for increasing soil fertility.

3.4. Characterization of Biochar. *3.4.1. SEM.* Biochar surface morphology and structural features were examined with the aid of SEM images regarding porosity. The SEM images were captured at various resolutions to compare the samples on different scales. The pyrolysis process at different calcination temperatures resulted in minimal (cracks and holes) morphological changes in biochar (Figure 3) and the formation of volatiles, whereas the degree of devolatilization significantly influences biochar properties. These porous structures are heterogeneous because it is formed due to the shrinkage and the flow of volatile matter.[22] The biochar porosity is enhanced upon elevating the temperature of pyrolysis, which explains the high porosity in all the biochar produced at 350 °C except GS350. The pores were irregular and robust configuration.[23] The large irregularity in the porosity of RH250 may be due to incomplete decomposition of feedstocks at 250 °C, whereas RH300 and RH350 show a pore network that is well defined and more uniform as the large pores shrink and become smaller. A relatively low pyrolytic temperature is linked to incomplete decomposition in SB250, resulting in the formation of a few pores. The feedstocks undergo proper thermal degradation at pyrolytic temperatures of 300 and 350 °C; therefore, the biochar samples SB300 and SB350 have more pores. GS250 also has a minimal porous structure due to insufficient degradation, whereas GS300 has more well-defined pores, indicating significant degradation of feedstocks. The GS350 sample has a damaged and colloidal pore structure due to the over-degradation of feedstock at 350 °C. While alterations in pore structure can be seen with rising temperatures, the variations are not substantial given the limited range of pyrolysis

https://doi.org/10.1021/acsomega.5c00120
ACS Omega XXXX, XXX, XXX−XXX

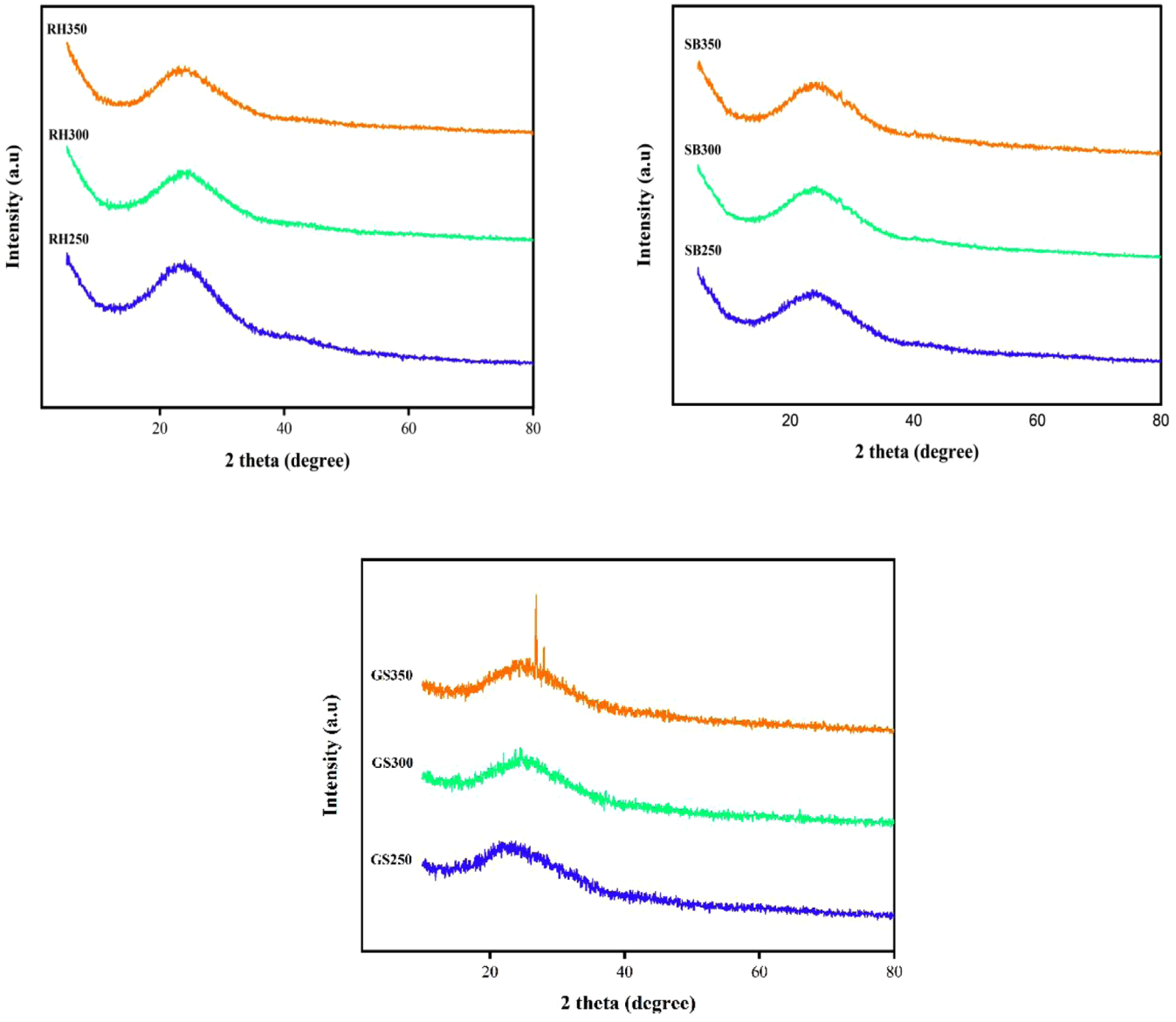

Figure 5. XRD characterization of biochar samples at different temperatures.

temperatures (250−350 °C), which may not be adequate to trigger significant structural changes, especially in dense materials such as groundnut shells. This indicates that the loss of porosity and surface structure of the biochar sample can occur due to both incomplete and overfeedstock decomposition.[35−37] SEM analysis outcomes were aligned with the previous study by Liu et al.,[29] which revealed well-defined porous structures in biochar with increasing pyrolysis temperature. It emphasizes that temperature plays a vital role in influencing important morphological characteristics such as porosity and surface structure, which have a direct effect on the efficacy of biochar in various applications like adsorption (due to increased surface area), soil amendment (by enhancing physical structure and water retention), and catalysis (by improving the availability of active sites).[25,33,38]

3.4.2. FTIR. A broad peak was observed at around 3100−3600 cm^{-1} in all biochar samples, corresponding to OH stretching (Figure 4). These peaks represent the phenols and alcohols from the hydroxyl functional groups or adsorbed water.[39] A narrow peak was identified at 2108 and 2097 cm^{-1} in RH and SB, representing the presence of N═C═S stretching characteristic of isothiocyanate. This indicates the formation of sulfur and nitrogen during the pyrolysis of the organic raw materials. The small peaks at 1711, 1713, and 1714 cm^{-1} present in RH, SB, and GS correspond to the carboxylic acids' C═O stretching vibration.[18] The peaks at 1602, 1579, and 1584 cm^{-1} show that cyclic alkenes are stretching their C═C bonds, and a peak at 1373 cm^{-1} corresponds to the presence of symmetric stretching of nitro compounds, NO_2.[40,41] The C−H bending present in GS biochar, marked by the peak at 1393 cm^{-1}, indicates methylene groups. The peaks at 1114 and 1121 cm^{-1} show C−O stretching associated with aliphatic ethers,[42] while at 1056 cm^{-1} corresponds to C−O stretching of primary ethers, confirming the presence of hemicellulose.[43] The peak at 872 cm^{-1} is attributed to ═C−H (aromatic) stretching vibration.[44] The peak at 797 cm^{-1} indicates C═C bending associated with alkali, and peaks at 757 cm^{-1} and 759 cm^{-1} are attributed to C−C bending.[45] The 681 cm^{-1} peak signifies the C−Br stretching of aliphatic bromine compounds. Spectral bands below 600 cm^{-1} originate

https://doi.org/10.1021/acsomega.5c00120
ACS Omega XXXX, XXX, XXX−XXX

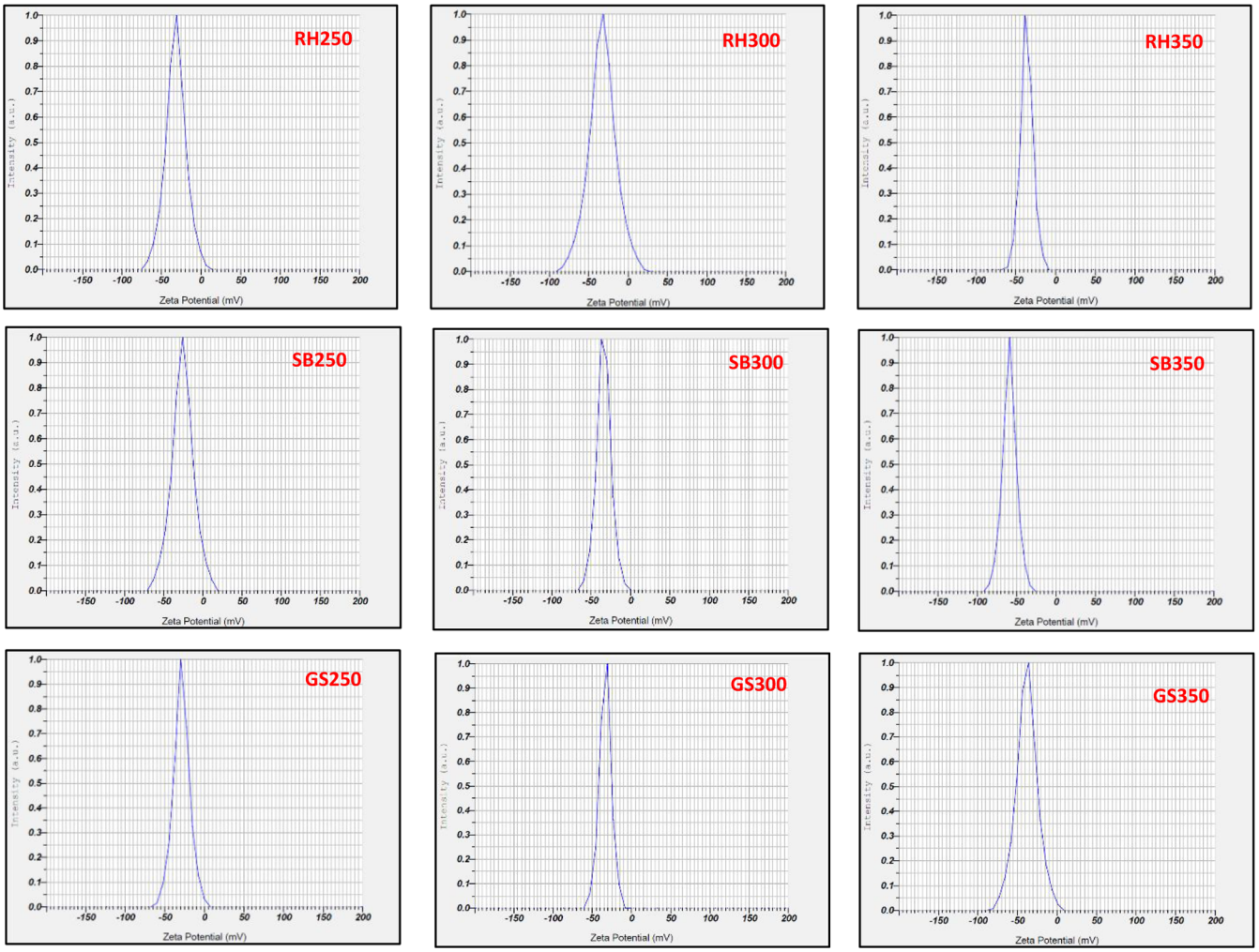

Figure 6. ζ-Potential analysis of biochar samples.

from stretching vibrations associated with organic and inorganic halogen compounds. The variations in the infrared spectra at different temperatures indicate water loss, the combustion of organic compounds, and an increase in the proportion of mineral components in the biochar.[46] This functional transformation shows variation with temperature and aligns with the FTIR patterns reported by Ray et al.,[42] where enhanced pyrolysis contributed to the degradation of easily broken compounds while maintaining thermally stable aromatic and carboxylic groups.

3.4.3. XRD. The XRD pattern of RH, SB, and GS biochar prepared at three different temperatures, 250, 300, and 350 °C, exhibited a broad hump in the low-angle region (2θ = 15−35°) (Figure 5) due to the (002) stacking of the graphite base planes. Biochar was predominantly amorphous with crystalline features associated with the graphite phase, improving its porosity and absorption capacity.[47,48] Furthermore, no other characteristic peaks were detected in all spectra except for those of GS350. Sample GS350 shows a prominent peak at 2θ = 26.7, indicating that SiO_2 is present in its crystalline form and that biochar decomposes at elevated temperatures. The most prominent crystallographic structure within biochar is formed from the cellular crystallinity, whereas the presence of turbostratic crystallites in the structure.[49−52]

4. ζ-POTENTIAL

The ζ-potential gradually increases from −32.0 to −36.4 mV at 250 and 350 °C, respectively, for rice husk biochar, whereas, in the instance of sugarcane bagasse, a substantial change has been noticed, ranging from −26.1 to −59.3 mV at 250 and 350 °C (Figure 6). This indicates that it undergoes significant chemical changes at higher temperatures, producing a high surface charge with increased adsorption potential. Therefore, the stability is moderate (SB250 and SB300) and good (SB350). A similar pattern to that of rice husk has been observed in groundnut shell biochar, exhibiting a gradual increase from 29.1 to −38.1 mV at 250 and 350 °C, respectively, indicating a moderate stability improvement in surface activity with an increase in temperature.[39] The results show that the value of the ζ-potential becomes more negative with increasing temperature. Biochars produced at high temperatures have more negative surface charge, which enhances their interactions more electrostatically with positively charged ions such as heavy metals, nutrients, and pollutants.[53,54] These properties render high-temperature biochar more effective for soil remediation and wastewater treatment. Furthermore, the development of more negative charges on biochar repels each other by reducing aggregation and improving biochar dispersion.[55,56]

https://doi.org/10.1021/acsomega.5c00120
ACS Omega XXXX, XXX, XXX−XXX

5. CONCLUSIONS

The impact of various temperatures of pyrolysis on the biochar physicochemical characteristics synthesized from three distinct raw materials (rice husks, sugarcane bagasse, and groundnut shell) reveals that raising temperatures led to a decrease in yield and moisture content as a consequence of augmented thermal degradation, thereby signifying an improvement in carbonization. An increase in the pH, EC, ash, and fixed carbon was evident with a spike in the temperature, indicating the presence of inorganic minerals and soluble salts. These modifications improve the alkalinity and enrich the nutrient content of the biochar, making it an effective means of improving soil and trapping pollutants. The highest biochar yield (44.63%) was observed in RH250 compared to the other samples. The highest pH (7.7) and EC (4.567) values were observed in RH350 and SB350, respectively. In proximate analysis, the highest ash (39.12%), moisture (13.6%), fixed carbon (82.4%), and volatile matter (30.7%) values were observed in RH350, SB250, GS350, and RH250, respectively. The observed trends suggest that elevated levels of ash and fixed carbon enhance the structural integrity, improve resistance to deterioration, and boost the adsorption capacity, which are the parameters essential for effective long-term carbon sequestration. CHNS analysis shows a spike in the carbon value with the elevating temperature of pyrolysis, thereby indicating stronger charring. The highest carbon content (75.56%) was found at GS350, whereas nitrogen and hydrogen diminished with higher pyrolysis temperatures. The observed decrease in hydrogen and oxygen concentrations with increasing temperature corresponds with standard devolatilization patterns, improving the aromatic properties, thermal stability, and reduced polarity of the biochar matrix. The ICP-MS data showed that the concentrations of minerals, such as potassium, calcium, and magnesium, increase in the biochar obtained from GS and SB, especially at higher temperatures, suggesting that it could be used as a soil amendment. The type of biomass and the temperature used in pyrolysis had a considerable impact on the structure and morphology of the produced biochar, as demonstrated by SEM analysis. The SEM images show that the ideal temperature has a well-defined structure, especially at 300 °C and 350°, for all of the samples, which improves the soil physical properties and absorption capacity of the biochar. All the biochar samples have the same surface functional groups, and a significant change was noticed with the increase in temperature, showing a defined structure of −OH, −COOH, and aromatic functional groups. Furthermore, XRD confirmed the presence of amorphous and crystalline silica structures at various temperatures. ζ-potential increased upon increasing the temperature and became more negative at 350 °C for all samples. It promotes the dispersion stability and electrostatic interaction with cations including impurities such as heavy metals, nutrients, and pollutants. In summary, biochar produced at moderate to high temperatures, particularly at 350 °C, exhibits improved physicochemical and structural properties that make it a significant and sustainable resource for environmental management. Further long-term soil experiments are recommended to confirm its effectiveness in improving soil health, nutrient availability, and pollutant removal compared with conventional soil amendments.

AUTHOR INFORMATION

Corresponding Author

Saiyyeda Firdous − *VIT School of Agricultural Innovations and Advanced Learning, Vellore Institute of Technology (VIT), Vellore 632 014, India;* orcid.org/0000-0001-6588-1556; Email: saiyyeda.firdous@vit.ac.in

Author

Kowsalya Sathyabama − *VIT School of Agricultural Innovations and Advanced Learning, Vellore Institute of Technology (VIT), Vellore 632 014, India*

Complete contact information is available at: https://pubs.acs.org/10.1021/acsomega.5c00120

Author Contributions

The manuscript was written through contributions of all authors. All authors have given approval to the final version of the manuscript.

Notes

Ethical approval declaration is not applicable to this article. The authors declare no competing financial interest.

ACKNOWLEDGMENTS

The authors acknowledge VIT, Vellore, for providing XRD, FTIR, SEM, ζ-potential, and PURSE VIT, for providing ICP-MS facilities.

REFERENCES

(1) Gatkal, N. R.; Nalawade, S. M.; Sahni, R. K.; Walunj, A. A.; Kadam, P. B.; Bhanage, G. B.; Datta, R. Heliyon Present trends, sustainable strategies and energy potentials of crop residue management in India : A review. *Heliyon* **2024**, *10* (21), No. e39815.

(2) Jain, N.; Bhatia, A.; Pathak, H. Emission of Air Pollutants from Crop Residue Burning in India. *Aerosol Air Qual. Res.* **2014**, *14*, 422−430.

(3) Sarangi, P. K.; Sahoo, H. P.*Agricultural Crop Residues: Unutilized Bio- mass Having Huge Energy Creation Potential.* 2013; Vol. *4* 12, pp 152−154.

(4) Sahoo, S. S.; Vijay, V. K.; Chandra, R.; Kumar, H. Production and characterization of biochar produced from slow pyrolysis of pigeon pea stalk and bamboo. *Cleaner Eng. Technol.* **2021**, *3*, No. 100101.

(5) Venkatramanan, V.; Shah, S.; Rai, A. K.; Prasad, R. Nexus Between Crop Residue Burning, Bioeconomy and Sustainable Development Goals Over North-Western India. *Front. Energy Res.* **2021**, *8*, No. 614212.

(6) Pariyar, P.; Kumari, K.; Jain, M. K.; Jadhao, P. S. Evaluation of change in biochar properties derived from different feedstock and pyrolysis temperatures for environmental and agricultural applications. *Sci. Total Environ.* **2020**, *713*, No. 136433.

(7) Bera, T.; Purakayastha, T. J.; Patra, A. K.; Datta, S. C. Comparative analysis of physicochemical, nutrient, and spectral properties of agricultural residue biochars as influenced by pyrolysis temperatures. *J. Mater. Cycles Waste Manage.* **2018**, *20* (2), 1115−1127.

(8) Rehrah, D.; Reddy, M. R.; Novak, J. M.; Bansode, R. R.; Schimmel, K. A.; Yu, J.; Watts, D. W.; Ahmedna, M. Production and characterization of biochars from agricultural by-products for use in soil quality enhancement. *J. Anal. Appl. Pyrolysis* **2014**, *108*, 301−309.

(9) Dejene, D.; Tilahum, E. Characterization of Biochar Produced from Different Feed Stocks for Waste Management. *Int. J. Environ. Sci. Nat. Resour.* **2019**, *20* (3), No. 556040, DOI: 10.19080/IJESNR.2019.20.556040.

(10) Cely, P.; Gascó, G.; Paz-ferreiro, J.; Méndez, A. Journal of Analytical and Applied Pyrolysis Agronomic properties of biochars

from different manure wastes. *J. Anal. Appl. Pyrolysis* **2015**, *111*, 173−182.
(11) Amalina, F.; Syukor, A.; Razak, A.; Krishnan, S.; Sulaiman, H.; Zularisam, A. W.; Nasrullah, M. Journal of Hazardous Materials Advances Biochar Production Techniques Utilizing Biomass waste-derived materials and environmental applications − A review. *J. Hazard. Mater. Adv.* **2022**, *7*, No. 100134.
(12) Ganesapillai, M.; Mehta, R.; Tiwari, A.; Sinha, A. Heliyon Waste to Energy : A review of biochar production with emphasis on Mathematical modeling and its applications. *Heliyon* **2023**, *9* (4), No. e14873.
(13) Yaashikaa, P. R.; Kumar, P. S.; Varjani, S.; Saravanan, A. A critical review on the biochar production techniques, characterization, stability, and applications for circular bioeconomy. *Biotechnol. Rep.* **2020**, *28*, No. e00570.
(14) Nartey, O. D.; Zhao, B. Biochar Preparation, Characterization, and Adsorptive Capacity and Its Effect on Bioavailability of Contaminants: An Overview. *Adv. Mater. Sci. Eng.* **2014**, *2014*, No. 715398, DOI: 10.1155/2014/715398.
(15) Li, S.; Harris, S.; Anandhi, A.; Chen, G. Predicting biochar properties and functions based on feedstock and pyrolysis temperature : A review and data syntheses. *J. Cleaner Prod.* **2019**, *215*, 890−902.
(16) Tomczyk, A.; Sokołowska, Z.; Boguta, P. Biochar physicochemical properties: pyrolysis temperature and feedstock kind effects. *Rev. Environ. Sci. Biotechnol.* **2020**, *19* (1), 191−215.
(17) Khater, E. S.; Bahnasawy, A.; Hamouda, R.; Sabahy, A.; Abbas, W.; Morsy, O. M. Biochar production under different pyrolysis temperatures with different types of agricultural wastes. *Sci. Rep.* **2024**, *14*, No. 2625.
(18) Dhar, S. A.; Sakib, T. U.; Hilary, L. N. Effects of pyrolysis temperature on production and physicochemical characterization of biochar derived from coconut fiber biomass through slow pyrolysis process. *Biomass Convers. Biorefin.* **2022**, *12*, 2631−2647.
(19) Goskula, S.; Siliveri, S.; Gujjula, S. R.; Chirra, S.; Narayanan, V. Synthesis of Sustainable Acid Biochar Catalysts Derived from Waste Biomass for Esterification of Glycerol. *ChemistrySelect* **2023**, *8*, No. e202203662, DOI: 10.1002/slct.202203662.
(20) Kumar, N. V.; Sawargaonkar, G.; Rani, C. S.; Pasumarthi, R.; Kale, S.; et al. Harnessing the potential of pigeonpea and maize feedstock biochar for carbon sequestration, energy generation, and environmental sustainability. *Bioresour. Bioprocess.* **2024**, *11*, No. 5, DOI: 10.1186/s40643-023-00719-3.
(21) Aller, D.; Bakshi, S.; Laird, D. A. Journal of Analytical and Applied Pyrolysis Modified method for proximate analysis of biochars. *J. Anal. Appl. Pyrolysis* **2017**, *124*, 335−342.
(22) Zhang, M.; Peng, F.; Yu, J.; Liu, Z. Feedstock-Induced Changes in the Physicochemical Characteristics of Biochars Produced from Different Types of Pecan Wastes. *Forests* **2024**, *15*, No. 366, DOI: 10.3390/f15020366.
(23) Mishra, R. K.; Kumar, D. J. P.; Narula, A.; Chistie, S. M. Production and beneficial impact of biochar for environmental application : A review on types of feedstocks, chemical compositions, operating parameters, techno-economic study, and life cycle assessment. *Fuel* **2023**, *343*, No. 127968.
(24) Noor, N. M.; Shariff, A.; Abdullah, N.; Syairah, N. S. M. Temperature effect on biochar properties from slow pyrolysis of coconut flesh waste. *Malays. J. Fundam. Appl. Sci.* **2019**, *15* (2), 153−158.
(25) Roshan, A.; Ghosh, D.; Maiti, S. K. How temperature affects biochar properties for application in coal mine spoils ? A meta - analysis. *Carbon Res.* **2023**, *2*, No. 3.
(26) Conz, R. F.; Abbruzzini, T. F.; de Andrade, C. A.; Milori, D. M. B. P.; Cerri, C. E. P. *Effect of Pyrolysis Temperature and Feedstock Type on Agricultural Properties and Stability of Biochars* **2017**, *8*, 914−933.
(27) Li, S.; Harris, S.; Anandhi, A.; Chen, G. Predicting biochar properties and functions based on feedstock and pyrolysis temperature : A review and data syntheses. *J. Cleaner Prod.* **2019**, *215*, 890−902.
(28) Zhang, M.; Peng, F.; Yu, J.; Liu, Z. Feedstock-Induced Changes in the Physicochemical Characteristics of Biochars Produced from Different Types of Pecan Wastes. *Forests* **2024**, *15*, No. 366, DOI: 10.3390/f15020366.
(29) Liu, Z.; Zhang, Y.; Liu, Z. Bioresource Technology Comparative production of biochars from corn stalk and cow manure. *Bioresour. Technol.* **2019**, *291*, No. 121855.
(30) Sun, H.; Zhang, H.; Xiao, H.; Shi, W.; Müller, K.; Van Zwieten, L.; Wang, H. Wheat straw biochar application increases ammonia volatilization from an urban compacted soil giving a short-term reduction in fertilizer nitrogen use efficiency. *J. Soils Sediments* **2019**, *19*, 1624−1631.
(31) Novak, J. M.; Lima, I.; Gaskin, J. W.; Steiner, C.; Das, K. C.; Ahmedna, M.; Watts, D. W.; Warren, J.; Schomberg, H. Characterization of designer biochar produced at different temperatures and their effects on a loamy sand. *Ann. Evniron. Sci.* **2009**, *3* (843), 195−206.
(32) Jindo, K.; Mizumoto, H.; Sawada, Y.; Sonoki, T. Physical and chemical characterization of biochars derived from. *Biogeosciences* **2014**, *11*, 6613−6621.
(33) Xiao, X.; Chen, Z.; Chen, B. H/C atomic ratio as a smart linkage between pyrolytic temperatures, aromatic clusters and sorption properties of biochars derived from diverse precursory materials. *Sci. Rep.* **2016**, *6*, No. 22644, DOI: 10.1038/srep22644.
(34) Claoston, N.; Samsuri, A. W.; Husni, M. H. A.; Amran, M. S. M. Effects of pyrolysis temperature on the physicochemical properties of empty fruit bunch and rice husk biochars. *Waste Manage. Res.* **2015**, *32*, 331−339, DOI: 10.1177/0734242X14525822.
(35) Burachevskaya, M.; Minkina, T.; Bauer, T.; Lobzenko, I.; Fedorenko, A.; Mazarji, M.; Sushkova, S.; Mandzhieva, S.; Nazarenko, A.; Butova, V.; Wong, M. H.; Rajput, V. D. Fabrication of biochar derived from different types of feedstocks as an efficient adsorbent for soil heavy metal removal. *Sci. Rep.* **2023**, *13*, No. 2020.
(36) Estela, M. C. C. B.; Juliana, S.; Matos, T. T. S.; Mayara, R. F. Effect of surface and porosity of biochar on water holding capacity aiming indirectly at preservation of the Amazon biome. *Sci. Rep.* **2018**, *2017*, No. 10677.
(37) Peiris, C.; Nayanathara, O.; Navarathna, C. M.; Jayawardhana, Y.; Nawalage, S.; Burk, G.; Karunanayake, A. G.; Madduri, S. B.; Vithanage, M.; Kaumal, M. N.; Mlsna, T. E.; Hassan, E. B.; Abeysundara, S.; Ferez, F.; Gunatilake, S. R. The influence of three acid modifications on the physicochemical characteristics of tea-waste biochar pyrolyzed at different temperatures: A comparative study. *RSC Adv.* **2019**, *9* (30), 17612−17622.
(38) Sarkar, D.; Panicker, T. F.; Mishra, R. K.; Kini, M. S. A comprehensive review of production and characterization of biochar for removal of organic pollutants from water and wastewater. *Water-Energy Nexus* **2024**, *7*, 243−265.
(39) Claoston, N.; Samsuri, A. W.; Husni, M. H. A.; Amran, M. S. M. Effects of pyrolysis temperature on the physicochemical properties of empty fruit bunch and rice husk biochars. *Waste Manage. Res.* **2015**, *32*, 331−339, DOI: 10.1177/0734242X14525822.
(40) Mary, G. S.; Niveditha, P.; Niveditha, S.; et al. Production, characterization and evaluation of biochar from pod (Pisum sativum), leaf (Brassica oleracea) and peel (Citrus sinensis) wastes. *Int. J. Recycl.Org. Waste Agric.* **2016**, *5* (1), 43−53.
(41) Nanda, S.; Mohanty, P.; Pant, K. K.; et al. Characterization of North American Lignocellulosic Biomass and Biochars in Characterization of North American Lignocellulosic Biomass and Biochars in Terms of their Candidacy for Alternate Renewable Fuels. *BioEnergy Res.* **2012**, *6*, 663−677, DOI: 10.1007/s12155-012-9281-4.
(42) Ray, A.; Banerjee, A.; Dubey, A. Characterization of Biochars from Various Agricultural By- Products Using Characterization of Biochars from Various Agricultural By- Products Using FTIR Spectroscopy, SEM focused with image Processing. *Int. J. Agric. Enviorn. Biotechnol.* **2020**, *13*, 423−430, DOI: 10.30954/0974-1712.04.2020.6.
(43) Kurian, J. K.; Gariepy, Y.; Orsat, V.; Raghavan, G. S. V. Microwave-assisted lime treatment and recovery of lignin from

https://doi.org/10.1021/acsomega.5c00120
ACS Omega XXXX, XXX, XXX−XXX

hydrothermally treated sweet sorghum bagasse. *Biofuels* **2015**, *6*, 341−355, DOI: 10.1080/17597269.2015.1110775.
(44) Kumar, R.; Kumar, M.; Awasthi, K. Selective deposition of Pd nanoparticles in porous PET membrane for hydrogen separation. *Int. J. Hydrogen Energy* **2017**, *42* (22), 15203−15210.
(45) Bicchieri, M.; Piantanida, G.; Sodo, A. Non-destructive spectroscopic investigation on historic Yemenite scriptorial fragments: Evidence of different degradation and recipes for iron tannic inks. *Anal. Bioanal. Chem.* **2013**, *405*, 2713−2721, DOI: 10.1007/s00216-012-6681-4.
(46) Mishra, R. K.; Kumar, V.; Mohanty, K. Pyrolysis kinetics behaviour and thermal pyrolysis of Samanea saman seeds towards the production of renewable fuel. *J. Energy Inst.* **2020**, *93* (3), 1148−1162.
(47) Alshammari, H. M.; Abbas, N. Effect of Pyrolysis Temperature during Valorization of Date Stones on Physiochemical Properties of Activated Carbon and Its Catalytic Activity for the Oxidation of Cycloalkenes. *Catalysts* **2021**, *11*, No. 686, DOI: 10.3390/catal11060686.
(48) Guo, F.; Jiang, X.; Li, X.; Peng, K.; Guo, C.; Rao, Z. Carbon electrode material from peanut shell by one-step synthesis for high-performance supercapacitor. *J. Mater. Sci.: Mater. Electron.* **2019**, *30* (1), 914−925.
(49) Burachevskaya, M.; Minkina, T.; Bauer, T.; Lobzenko, I.; Fedorenko, A.; Mazarji, M.; Sushkova, S.; Mandzhieva, S.; Nazarenko, A.; Butova, V.; Wong, M. H.; Rajput, V. D. Fabrication of biochar derived from different types of feedstocks as an efficient adsorbent for soil heavy metal removal. *Sci. Rep.* **2023**, *13*, No. 2020.
(50) Liu, Y.; Zhao, X.; Li, J.; et al. Desalination and Water Treatment Characterization of bio-char from pyrolysis of wheat straw and its evaluation on methylene blue adsorption. *Desalin. Water Treat.* **2016**, *46*, 115−123, DOI: 10.1080/19443994.2012.677408.
(51) Alsharef, J. M. A.; Taha, M. R.; Khan, T. A. Physical dispersion of nanocarbons in *J. Teknol.* 2017; Vol. *79* DOI: 10.11113/jt.v79.7646.
(52) Rambhatla, N.; Florence, T.; Kumar, R.; Kini, S.; Sharma, A. Results in Engineering Biomass pyrolysis for biochar production : Study of kinetics parameters and effect of temperature on biochar yield and its physicochemical properties. *Results Eng.* **2025**, *25*, No. 103679.
(53) El-Gamal, E. H.; Reshad, M.; Saleh, M. E.; et al. Potential bioremediation of lead and phenol by sunflower seed husk and rice straw - based biochar hybridized with bacterial consortium : a kinetic study. *Sci. Rep.* **2023**, *13*, No. 21901.
(54) Mansee, A. H.; Abdelgawad, D. M.; Gamal, E. H.; El-Gamal, E. H.; Ebrahim, A. M.; Saleh, M. E. Influences of Mg - activation on sugarcane bagasse biochar characteristics and its PNP removing potentials from contaminated water. *Sci. Rep.* **2023**, *13*, No. 19153.
(55) Hong, M.; Zhang, L.; Tan, Z. Effect mechanism of biochar's zeta potential on farmland soil 's cadmium immobilization. *Environ. Sci. Pollut. Res.* **2019**, *26*, 19738−19748.
(56) Hosny, M.; Fawzy, M.; Eltaweil, A. S. Green synthesis of bimetallic Ag/ZnO @ Biohar nanocomposite for photocatalytic degradation of tetracycline, antibacterial and antioxidant activities. *Sci. Rep.* **2022**, *12*, No. 7316.

https://doi.org/10.1021/acsomega.5c00120
ACS Omega XXXX, XXX, XXX−XXX